IEEE Transactions on Nuclear Science, Vol. NS-32, No. 5, October 1985

MODELLING THE TRIUMF RF CAVITY USING THE CODE RFQ3D

D. Dohan, K. Fong and R. Hutcheon†
TRIUMF, Vancouver, B.C., Canada V6T 2A3

Summary

Development work on the TRIUMF cyclotron RF cavity requires an efficient code to study the effects on voltage distributions of resonator geometry non-uniformity, including misalignment of the cantilevered cavity walls, the end flux guides and the centre post. A quasi-three-dimensional code, RFQ3D, although originally written for radio frequency quadrupole cavity studies, has been successfully adapted to simulate the TRIUMF cavity.

The code uses four one-dimensional coupled transmission line equations to calculate the voltage distributions along the dee gap and allows for local variations in the transmission line inductance and capacitance. The effects of individual resonator components on the accelerating voltage profile and the RF leakage for both the fundamental and third harmonic frequencies are calculated and compared with precise 1:10 model measurements.

Introduction

The TRIUMF RF cavity[1] consists of 2 opposing dee's, each 3 meters wide by 16 meters long. The accelerating RF voltage is generated along the dee tips, which are supported 0.1 meters from the ground plane by individually cantilevered resonator segments (a total of 80 in all). Misalignments, distortions and vibrations of these segments are inevitable even under optimal operating conditions. In order to calculate the effects of these cavity perturbations on the characteristics of this unusually flat cavity, an efficient three-dimensional RF cavity code is required which can handle both large dimensions and small geometry perturbations. The presently available true 3-d computer RF cavity codes are either unable to cope with the TRIUMF geometry or consume an unacceptable amount of computational time.

RFQ3D[2] is a quasi-three-dimensional program originally written to calculate the effects of dimensional variations on the full three-dimensional properties of a radio frequency quadrupole cavity. The code treats an RFQ cavity as a system of four longitudinally continuously coupled 1-dimensional loaded transmission lines with appropriate boundary conditions. The radial dimensions of each lobe of the RFQ cavity is represented in the code by distributed transmission line shunt capacitances and inductances. Voltage and current profiles are calculated along the axis of the cavity which may have local variations in cross-sectional area. When used with values of equivalent distributed and lumped capacitance and inductance derived entirely from the cavity geometry, the code has successfully determined voltage distributions and resonance frequencies in the TRIUMF resonator. Non-uniformities along the dee gap such as flux guides, the centre post and misalignments of hot and/or ground arms can be simulated and their effects studied, at both the fundamental resonant frequency of 23 MHz and the third harmonic frequency of 69 MHz.

Calculation of distributed impedances (fundamental resonance)

The representation of the TRIUMF resonator structure as a grossly flattened RFQ is shown in Fig. 1. Probe housings attached to the tank lid and bottom

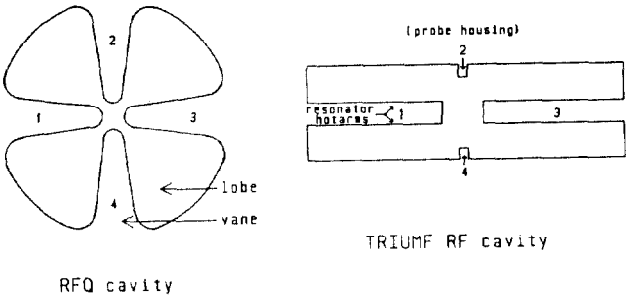

Fig. 1. Representation of the TRIUMF RF cavity as an RFQ (end view).

along the dee gap form two of the the RFQ vanes (2 and 4), whereas the dee hot arms, in which the upper and lower tips are assumed for this study to be connected, form vanes 1 and 3.

At resonance, each RFQ lobe can be represented by a quarter wave stub at 23 MHz (three-quarter wave at 69 MHz) that is shorted at one end and capacitively loaded at the dee gap. The dee tip capacitance per unit length consists of 2 parts: the tip-to-tip capacitance C_{tt} and the tip-to-probe housing capacitance C_{tp}. Due to their complex geometries, C_{tp} and C_{tt} are evaluated using numerical methods. Using SUPERFISH the following values are obtained:

$$C_{tp} = 6.9 \text{ pF/m}$$
$$C_{tt} = 10.6 \text{ pF/m}$$

The corresponding equivalent lumped element circuit is given in Fig. 2. The total "vane-to-vane" capacitance is equal to the sum of the transmission line capacitance C_o and the tip-to-probe housing capacitance C_{tp}:

$$C_i = C_o + C_{tp} \qquad i=1,2,3,4$$

To calculate C_o and L_o due to the transmission line, we first note that the capacitance and inductance per unit length for a parallel plate are

$$C = \varepsilon y/d$$

and

$$L = \mu y d$$

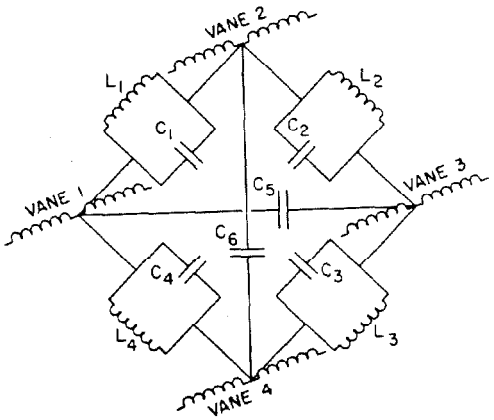

Fig. 2. Equivalent circuit of the RFQ model of the TRIUMF cavity.

†CRNL

0018-9499/85/1000-2933$01.00© 1985 IEEE

where y is the width of the plate, d is the distance between the plates, ε is the relative permittivity and μ is the relative permeablility. Since the current and the voltage in the line are distributed sinusoidally, the equivalent capacitance and inductance in a resonant line must be reduced from the dc parallel plate value. Their distributions at the frequencies of interest can be calculated using the total tip loading capacitance and the characteristic impedance of the transmission line. These average values can then be used to calculate the equivalent capacitance and inductance of the line. The resultant values are

$$L_o = 265.3\ \mu H/m$$
$$C_o = 161.5\ pF/m$$

The "vane-to-vane" capacitances are:

$$C_i = 168.4\ pF/m, \qquad i=1,2,3,4$$

The "cross-vane" capacitances C_5 and C_6 are given by

$$C_5 = C_{tt} = 10.6\ pF/m$$

and

$$C_6 = C_{pp} = 1.6\ pF/m$$

where C_{pp} is the probe housing-to probe housing capacitance and is calculated using a parallel plate approximation. The "cross-vane" inductances L_5 and L_6 are zero except at the centerpost region. Modifications to the above distributed values are necessary at the central region due to the centre post structure. Since the center post connects the top and the bottom probe housing together the equivalent reactance of this section of the line is given by the inductance of a cylinder,

$$L_5 = 0.0385\ nH$$

Structural features in the centre post region, including a pedestal and cutouts in the hot arms, are included in the distributed impedances of the transmission line as step functions with smooth edges and normalized to provide the correct integrated capacitance or inductance over the length of the centre post.

Finally, the equivalent lumped inductances and capacitances due to the flux guide and the tank side wall is evaluated. Because of the complex geometry of the flux lines, at best an estimate of the equivalent lumped elements can be given. Again assuming a sinusoidal distribution of voltages and current along the line, the L's and C's are given by

$$L_{ei} = 872.3\ nH \qquad i=1,3$$
$$L_{ej} = 101.3\ nH \qquad j=2,4$$
$$C_{ei} = 44.2\ \mu F$$
$$C_{ej} = 0.4\ \mu F$$

Due to the complex nature of the end region, the calculations for the lumped values of the equivalent impedances are approximate and are useful only in determining the effects of geometry changes, rather than for calculating the absolute magnitudes of voltages.

Calculation of distributed impedances (third harmonic resonance)

Normally, the equivalent circuit approach is used to calculate the properties of the fundamental resonance. To study the cavity response at the third harmonic frequency it is necessary to modify the equivalent distributed capacitances and inductances from their fundamental values. From the parallel plate area considerations, the new shunt capacitances and inductances are 1/3 of the fundamental values:

$$C_{i3} = C_i/3$$

and

$$L_{i3} = L_i/3 \qquad i=1,2,3,4$$

However, due to the presence of other shunt elements at the tips, further modifications to Ci's and Li's are necessary. The admittance of a shorted line of length ℓ is given by

$$Y = j/Z_o \cot(\omega\ell/c)$$

where Z_o is the characteristic impedance of the line, ω the angular frequency and c the speed of light. When ω is close to the fundamental resonant frequency ω_1, it can be expressed as

$$Y = j/Z_o\ \pi/2\ (\omega_1-\omega)/\omega_1$$

and when close to the third harmonic frequency ω_3 as

$$Y = j/Z_o\ 3\pi/2\ (\omega_3-\omega)/\omega_3$$

Note that the admittance sensitivity to frequency is three times higher at third harmonic frequency. In order to include this effect and at the same time keeping the resonant frequency ω_3 constant, the following corrections to the C's and L's are necessary:

$$C_{i3}' = 3\ C_{i3} = Ci$$

and

$$L_{i3}' = 1/3\ L_{i3} = Li/9. \qquad i=1,2,3,4$$

Voltage Profile along the Dee Gap

The above values of capacitances and inductances were used in the RFQ3D code to calculate the voltage distribution along the dee gap, shown in Fig. 3. The dee gap voltage profile obtained from the calculation at 23 MHz shows a slight decrease of voltage towards the outer segments (Fig.3). A drop of 4.2% (-0.4 dB) is observed between the centre and the outermost segments. A pronounced voltage drop of 78.2% (-13.2 dB) occurs at 69 MHz, due to the shorter wavelength. Measurements on the TRIUMF cyclotron and on the 1:10 scale model also give similar results. The calculations showed that this non-uniformity is due to two effects:

1). The perturbation at the central region causes the shunt inductance to decrease slightly due to the cutout for the centre post but it also adds a significant amount of extra capacitance between the hot arms and

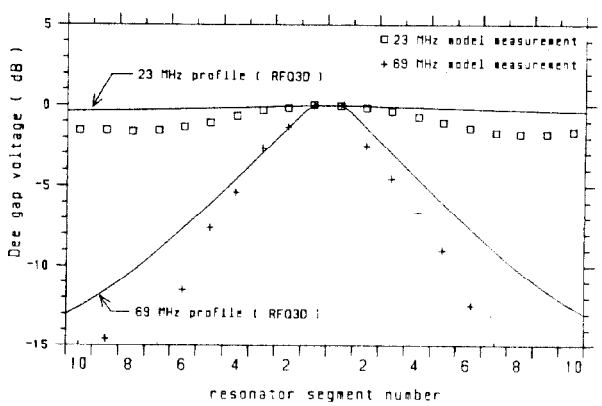

Fig. 3. Comparison of the RFQ3D calculations and measurements of the dee gap voltage profiles for both fundamental and third harmonic resonances.

the centre post structure. As a result the local resonant frequency in the centre region is lower than the rest of the resonator, resulting in a higher voltage at the centre.

2). At the flux guides there is very little tip loading capacitance. This and other geometry effects cause the local resonant frequency at the ends to be lightly higher than the rest of the resonator, resulting in a locally lower voltage at the ends.

These two effects combine to cause the observed voltage gradient along the dee gap. This gradient can be reduced or completely eliminated by reducing or compensating for the above two perturbations. Because the centre post is necessary for the injection of beam into the cyclotron, modification to the centre post geometry is not possible. However, the perturbation created by the post can be compensated by reducing the length of the central resonator segment at the shorted end of the transmission line. This is simulated in RFQ3D by reducing the inductance in the central region. Fig. 4 shows the changes of the voltage gradient as a function of the amount of shortening. At 23 MHz the shortening of the central resonator segments is all that is required to achieve an uniform voltage along the dee gap. At 69 MHz, however, the shorter wavelength allows voltage variation to occur over a much shorter distance, and adjustment at the outer regions (flux guides) is required to compensate for the perturbation at the flux guide.

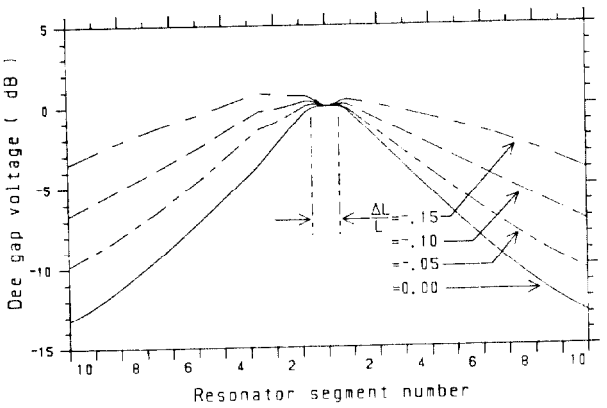

Fig. 4. RFQ3D calculations of the effect of central resonator shortening on the RF voltage profile (23 MHz).

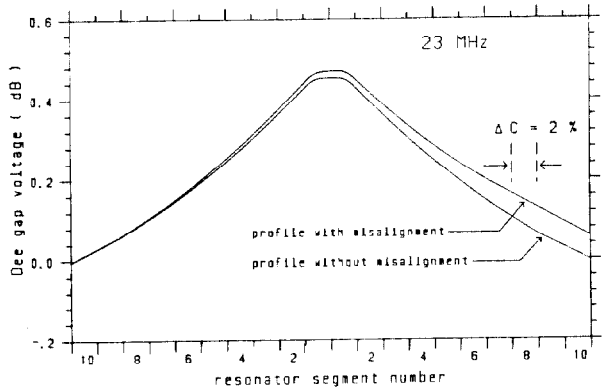

Fig. 5. Calculation of the effect of resonator misalignment on the 23 MHz voltage profile.

Effect of Resonator Misalignments

Since misalignments of the hot and ground arms mainly affect the geometry at the tip region where there is a strong electric field and a weak magnetic field, they can be simulated by a local change in the vane-to-vane capacitance. Fig. 5 shows the dee gap voltages when the equivalent capacitance of the cavity is increased by 2%, corresponding to a hot arm tip deflection of 3%.

In the figure the deflection occurs near the right end of vane 1, corresponding to segment 8, quadrant 1 of the cyclotron RF cavity. Voltage feedback regulation is simulated by renormalizing the result to the voltage at the left end of the vane (segment 10 of TRIUMF quadrant 2). The results show that the voltage profiles in this quadrant and along the length of vane 3 (TRIUMF quadrants 3 and 4) are not affected by the misalignment (less than 0.02 dB change), affected, i.e. only the distorted quadrant is affected by the distortion. The voltage on the distorted half quadrant changes by 0.7% (0.06 dB) and the other half quadrant changes by 0.5% (0.04 dB). This is in good agreement with the measurements on the cyclotron (0.09 dB) and in the 1:10 model. In the actual machine, vanes 1 and 3 are split into the upper and lower dee tips, which are however electrically connected at the flux guide ends of the dee gap.

These results showed that at the fundamental frequency of 23 MHz, the coupling between the upper and the lower quadrants through the flux guide is sufficiently strong that the perturbation in voltage due to misalignment in a quadrant will affect both the upper and the lower side of the quadrant. However, the presence of the centre post suppresses the propagation of the perturbation to the other quadrant of the same dee, and the dee-to-dee capacitance is too weak to allow propagation to the other dee.

The situation for the case of the third harmonic frequency is quite different, where the dee-to-dee coupling is now three time stronger due to the higher frequency. The perturbations due to the geometry distortion now are able to propagate to the both the upper and lower half of the opposite dee.

Conclusions

The results above were obtained using lumped and distributed impedances determined entirely from geometry considerations, and without fitting to RF voltage and frequency measurements. Comparison of the RFQ3D results with model and cyclotron measurements indicated that the code has sucessfully modelled the behavior of the TRIUMF cavity. It thus provided a valuable tool to identify the components in the cavity, such as the centre post and the flux guides, which have strong influences on the voltage profile in the dee gap. It also enables one to predict the behavior of the cavity when its geometry is changed.

Acknowlegements

The ideas and contribution of T. Enegren, D. Michelson and V. Pacak are gratefully acknowledged.

References

[1] R.L. Poirier and M. Zach, "TRIUMF RF system," IEEE Trans. Nucl. Sci. NS-22(3), 1253 (1975).
[2] R. Hutcheon, CRNL internal report, file no. 9022/ZEBRA-TM-34.